X-ray absorption fine structure study of the structural and electronic properties of the GdMg hydride switchable mirror

M. Di Vece,[1] A. M. J. van der Eerden,[2] J. A. van Bokhoven,[2,*] S. Lemaux,[2,†] J. J. Kelly,[1] and D. C. Koningsberger[2]
[1]*Debye Institute, Physics and Chemistry of Condensed Matter, Utrecht University, P.O. Box 80 000, 3508 TA Utrecht, The Netherlands*
[2]*Debye Institute, Inorganic Chemistry and Catalysis, Utrecht University, P.O. Box 80 083, 3508 TA Utrecht, The Netherlands*
(Received 23 July 2002; revised manuscript received 15 October 2002; published 31 January 2003)

Structural and electronic properties of the GdMg hydride switchable mirror have been studied with x-ray absorption fine structure (XAFS) spectroscopy at the Gd-L_3 edge. The analysis of the extended XAFS (EXAFS) data show phase segregation in the as-deposited film. The phase separation is enhanced by hydrogen intercalation. The structure of both the gadolinium clusters with low hydrogen concentration and the hydrogen-loaded gadolinium trihydride clusters is found to be hcp. EXAFS detected hydrogen atoms as scatterers, in a highly ordered structure. The structure of the gadolinium trihydride cluster is consistent with the model in which the hydrogen atoms are shifted from octahedral positions to the metal plane. The intensity of the Gd L_3 x-ray absorption edge increases after loading with hydrogen, pointing to a higher number of holes in the *d*-valence band. This suggests that a fraction of the available charge is transferred to the hydrogen atoms. This charge transfer is thought to be responsible for the optical change of the gadolinium thin film.

DOI: 10.1103/PhysRevB.67.035430 PACS number(s): 68.55.Jk, 61.10.Ht, 71.30.+h, 61.66.Dk

I. INTRODUCTION

Switchable mirrors, based on metal hydrides,[1] are interesting from a scientific and a technological point of view. The metal-insulator transition corresponding to a change from the optically opaque to the transparent state is an interesting phenomenon that can be applied in electro-optical devices.[2] This metal-insulator transition occurs by hydrogen intercalation with the metal going from the di- to trihydride state.

Yttrium and rare-earth metal hydride thin films show a yellow transmission in the transparent state. Alloying with magnesium provides a color-neutral switching device.[3,4] With higher magnesium content, the optical band gap increases. The rare-earth magnesium alloy with high magnesium content disproportionates under hydrogen loading, resulting in magnesium dihydride and rare-earth trihydride clusters.[4,5] The magnesium acts as a microscopic optical shutter; the magnesium metallic clusters are reflective while the insulating magnesium dihydride clusters allow good transmittance. It was proposed that magnesium switches at higher hydrogen concentrations than yttrium because of thermodynamic considerations. Observations by van der Molen *et al.*[6] show that yttrium trihydride stays fcc in yttrium magnesium alloys due to large stresses in the film caused by the relatively large magnesium to magnesium dihydride volume expansion. Recent research showed that magnesium nickel alloys also exhibit optical switching,[7] although the reflection and transmission contrasts are less than those of the rare-earth based switchable mirrors.

Band-structure calculations do not yield an unambiguous interpretation for the appearance of the band gap on hydrogen intercalation.[8] Different structural and electronic variations of the HoD_3 structure were proposed.[9] It is assumed that conduction electrons are captured by the hydrogen atoms, creating a negatively charged hydrogen ion in the tetrahedral and octahedral sites. Not all possible hydrogen positions are occupied. In the Kondo insulator model of Ng *et al.*,[10] the donated electron from a hydrogen vacancy is strongly localized. The Gutzwiller renormalization of the hydrogen band width results in the formation of a band gap. In the model of Kelly *et al.*,[11] a small displacement of the hydrogen atoms is considered to be responsible for the creation of a band gap. GW calculations by van Gelderen *et al.*[12] show that the existence of a band gap does not necessarily require symmetry lowering as proposed by Kelly *et al.*[11] However, a superposition of possible broken symmetry structures would result in the HoD_3 structure[13] preventing the detection of a broken symmetry structure.

Recent studies with IR spectroscopy[14] show that on average one electron is transferred to every two hydrogen atoms in $YH_{3-\delta}$. These results are not in line with the assumptions made in the band-structure calculations. The extent of charge transfer from the rare-earth atom, forming the host lattice, to the interstitial hydrogen atoms obviously remains a subject of debate. X-ray diffraction (XRD) studies suggest phase separation in the rare-earth Mg alloys by the detection of the separate element hydrides. The extent of phase separation is still unclear. Gadolinium magnesium alloy films with more than 50% magnesium are even XRD amorphous.[15] Therefore an investigation of the structure of rare-earth magnesium alloys on a local atomic scale could provide details about the structural anomalies. The lattice positions of hydrogen within the alloy or segregated thin film could yield more insight into the nature of the metal-insulator transition.

X-ray absorption fine structure (XAFS) is a technique well suited for determining structural and electronic properties of solids. The edge position is related to the oxidation state of the probed atom. From the x-ray absorption near-edge (XANES) region, information about the electronic structure and the medium-range order can be derived. EXAFS (extended x-ray absorption fine structure) provides information about the local structure, such as the nature and number of surrounding atoms and interatomic distances. No long-range order is required for XAFS spectroscopy.

In this study we have investigated GdMg polycrystalline films with XAFS spectroscopy at the Gd-L_3 edge in the as-deposited and fully hydrogenated states. Electronic information was extracted from the absorption edge shift and near-edge structure. From the EXAFS spectrum we have observed phase separation in the alloy. We were able to locate hydrogen directly as a scatterer in a lattice structure.

II. EXPERIMENT

A. Sample preparation

$Gd_{40}Mg_{60}$ polycrystalline layers were deposited on thin glass slides by evaporation at 10^{-7} mbar base pressure at a deposition rate of 1 nm/s. During pre-evaporation the metal vapor acts as a getter, reducing the ambient oxygen pressure considerably. For the sake of convenience the films will be denoted by GdMg. They are nominally 1-μm thick with a 50-nm caplayer of palladium The palladium serves as a catalyst for hydrogen dissociation and protects the film against oxidation. These GdMg films are similar to those described by Van der Sluis *et al.*[3]

B. Data collection

The XAFS spectra at the Gd-L_3 edge were obtained at the HASYLAB (Hamburg, Germany) beamline X1.1, which was equipped with a Si(311) double-crystal monochromator. All measurements were performed in a standard cell[16] in the transmission mode using ionization chambers filled with an Ar/N_2 mixture. Three stacked samples were used for a good signal-to-noise ratio. Measurements were performed on the as-deposited and fully hydrogen-loaded films. Loading of the samples to the ''trihydride'' state was achieved by applying a hydrogen flush at room temperature. The spectra were measured at 77 K. A gadolinium garnet powder XAFS spectrum was used to provide information on the edge position of gadolinium in the oxidized state.

C. Data analysis

The XDAP program developed by Vaarkamp *et al.*[17] was used for data analysis. Three scans were averaged during data reduction. The pre-edge background was approximated by a modified Victoreen function before subtraction.[18] The edge energy was determined with the maximum of the first derivative of the spectrum. The spectrum was background corrected with a cubic spline routine.[19] Normalization was performed by dividing the background of the absorption spectrum by the height of the absorption edge after 50 eV, leading to normalized EXAFS data.

Gd-Gd, Gd-Mg, Gd-O, and Gd-H references used for the fitting procedure were calculated with FEFF8.[20] The Gd-Gd and Gd-O references where calibrated with a Gd thin film and a garnet, respectively. A Hedin-Linquist potential[20] was used to calculate the phase shift and the backscattering amplitude. The crystallographic data and input parameters for FEFF used to create the EXAFS references are listed in Table I.

The difference file technique was applied together with Fourier transforms to resolve the different contributions in the EXAFS data.[21] If the experimental spectrum is composed of different contributions, then

TABLE I. Crystallographic data and input parameters for FEFF used to create the reference files.

Absorber-backscatterer	N	R (Å)	S_0^2	V_r (eV)	V_i (eV)
Gd-Gd	1	3.5	1	4.78	0
Gd-Mg	1	3.5	1	0	0
Gd-O	1	2.4	1	0	0
Gd-H	1	2	1	0	0

$$\text{expt. data} = \sum_{i=1}^{N} (\text{fit})_i , \tag{1}$$

where $(\text{fit})_i$ represents the fitted contribution of coordination shell *i*. For each individual contribution the following equation should then logically be valid:

$$(\text{fit})_j = \text{expt. data} - \sum_{i=1 \text{ and } i \neq j}^{N} (\text{fit})_i . \tag{2}$$

The right-hand side of Eq. (2) is further denoted as the difference file of shell *j* in which the noise is contained. A good fit is obtained only if the total fit and each individual contributing co-ordination shell describe correctly the experimental EXAFS and the difference file, respectively. In this way not only the total EXAFS fit, but also the individual fits of all separate contributions can be determined reliably. Optimization has also been performed with different powers of *k*. This enables a selectivity with respect to light (H) and heavy (Gd) scatterers during this procedure.

The EXAFS data-analysis program XDAP allows multiple-shell fitting in *R* space by minimizing the residuals between both the absolute and the imaginary part of the Fourier transforms (FT) of the data and the fit. *R*-space fitting has important advantages compared to the usual fitting in *k* space and is extensively discussed in a recent paper by Koningsberger *et al.*[21] The variances of the magnitude and the imaginary part of the Fourier transforms of fit and data were calculated according to

$$\text{variance} = \frac{\int \{k^n [\text{FT}^n_{\text{model}}(R) - \text{FT}^n_{\text{exp}}(R)]\}^2 dR}{\int [k^n \text{FT}^n_{\text{exp}}(R)]^2 dR} \times 100. \tag{3}$$

In this study the statistical significance of a contribution was checked by a comparison of the amplitude of $(\text{fit})_j$ with the noise level present in the difference file (the noise in the difference file is essentially the same as the noise in the experimental data).

The number of independent parameters (N_{ind}) was determined as outlined in the ''Reports on Standard and Criteria in XAFS Spectroscopy:'' [22]

$$N_{\text{ind}} = \frac{2 \Delta k \Delta R}{\pi} + 2. \tag{4}$$

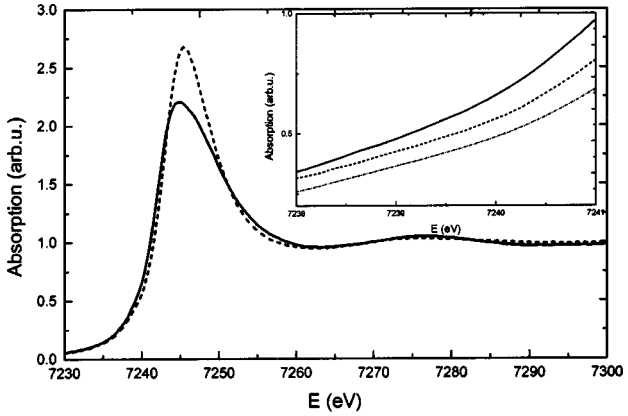

FIG. 1. The absorption spectra for the GdMg thin film in the as-deposited state (——) and after hydrogenation (- - -). In the inset the edge region is enlarged with the garnet spectrum included (-·-).

The accuracy of XAFS data analysis was considered by Koningsberger *et al.*,[21] in which the errors are estimated to be 5% in the coordination and 1% in the distance.

III. RESULTS

The normalized L_3 x-ray absorption near-edge spectra for the GdMg layers are shown in Fig. 1. It is clear that in the fully loaded state (dotted line), the intensity of the absorption edge has increased with respect to that of the virgin sample. This can be directly related to an increase in the number of holes in the *d* band. From the inset of Fig. 1, a shift of the edge to higher energy is also clearly observed. The difference between the energy at half maximum of the two absorption edge spectra is found to be 0.5 eV. This shift implies a positively charged gadolinium atom. The shift of the Gd edge position in garnet with respect to that of the metal is 0.9 eV.

Figure 2(A) shows the raw EXAFS data for the virgin sample (solid line) and the loaded film (dotted line). The loaded film has a significantly lower EXAFS amplitude than the virgin film. The virgin film exhibits a gradual decrease of the signal strength, while the loaded film shows a sudden decrease of the absorption after $k=4$, suggesting the dominant presence of a low *Z* scatterer (i.e., hydrogen). In Fig. 2(B) the k^0 weighed Fourier transforms of both EXAFS spectra are shown. The k^0 weighing has been chosen to emphasize the low-*k* region of the EXAFS spectrum, in which the hydrogen and oxygen contributions are dominant. The virgin film (solid line) peaks at 2.8 Å, with a much higher magnitude than the considerably smoother distribution of the loaded film (dotted line).

The k^0 weighed Fourier transform of the raw EXAFS data (solid line) of the as-deposited film together with the FT of the fit ($1<R<4$ Å) of the EXAFS spectrum (dotted line) are shown in Fig. 3. Four different scatterers, gadolinium, magnesium, oxygen, and hydrogen, had to be included in order to fit the data effectively. The fit matches the experimental data very well for values of *R* between 1.5 and 3.5 Å. Table II contains the resulting EXAFS coordination parameters. The

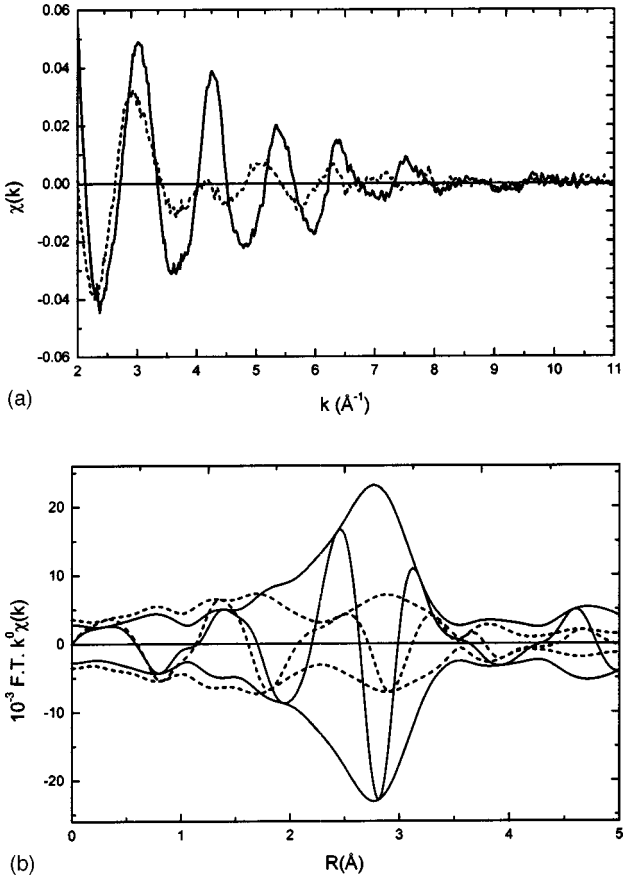

FIG. 2. (A) The EXAFS data after normalization and (B) The Fourier transform (k^0, $\Delta k=2.5-11$ Å^{-1}) for the as-deposited () and the hydrogenated (- - -) GdMg films.

Gd-Gd coordination number is three times larger than that of Gd-Mg. The total coordination (Gd plus Mg) around Gd is almost 12, while the Gd-Mg distance is about 0.22 Å smaller than the Gd-Gd distance. A small average number of oxygen and hydrogen neighboring atoms could also be detected around Gd with a coordination distance of 2.40 and 2.26 Å, respectively.

In Fig. 4(A), the k^0 weighed Fourier transform of the loaded film (solid line) is shown together with the best fit

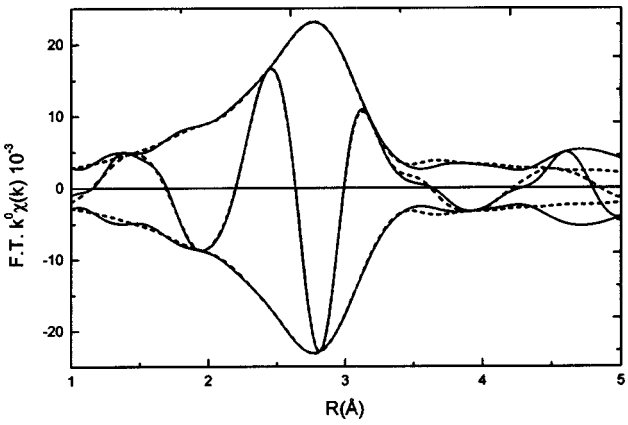

FIG. 3. Fourier transforms (k^0, $\Delta k=2.5-11$ Å^{-1}) of raw data (——) and fit (- - -) of the as deposited GdMg film.

TABLE II. Gd L_3 edge; sample $Gd_{40}Mg_{60}$/Pd as-synthesised; EXAFS analysis ($2.5<k<11$ Å^{-1}) k^0 weighing.

Absorber-backscatterer	N	R (Å)	$\Delta\sigma^2$ (10^{-3} Å^2)	ΔE_0 (eV)	k variance	
					imaginary	real
Gd-Gd	8.9	3.45	6.8	13.0	0.18	0.08
Gd-Mg	2.7	3.23	3.6	−5.1		
Gd-O	0.2	2.40	5.0	−7.0		
Gd-H	1.5	2.26	5.0	3.0		

($1<R<4$ Å) (dotted line). The absolute part of the transform shows two clear maxima at 1.7 and 2.9 Å, with a local minimum in between. This fit with the same four scatterers as detected for the virgin sample agrees well with the experimental data between 1 and 3.5 Å. The individual contributions to the fit as extracted with the difference file technique are plotted in Figs. 4(B)–(E). A well-defined single peak can be observed in Fig. 4(B) for the calculated Gd-Gd EXAFS at 2.9 Å (dotted line) and the corresponding difference file (solid line). The amplitude of the FT is about 70% of the amplitude of the FT of the total EXAFS spectrum [Fig. 4(A)]. In Fig. 4(C), the Gd-Mg EXAFS contribution (dotted line) and the corresponding difference file (solid line) are shown. A maximum can be located at 3.1 Å; however, the FT is distributed over a long range in R space due to a large Debye-Waller factor. The amplitude of the FT of the Gd-Mg contribution is about 15% of the amplitude of the FT of the total EXAFS. It is clear that the signal-to-noise (S/N) ratio of the FT of this Gd-Mg contribution is much lower than that of the FT of the Gd-Gd EXAFS. The Gd-O contribution (dotted line) and the corresponding difference file are displayed in Fig. 4(D). A clear peak is detected at around 1.9 Å. The maximum amplitude of the FT is 130% of the maximum amplitude at the same value of R in the FT of the total EXAFS signal. This points to an interference effect of the different EXAFS contributions. A very broad intense FT peak for the Gd-H contribution can be seen in Fig. 4(E). The maximum is located at 2.1 Å, with 80% of the total signal strength. The quality of the fit is good, confirming the detection of a hydrogen contribution. Inspection of Fig. 4 shows that the sum of the absolute signal strengths of the different contributions is higher than the total measured signal strength. Comparing Figs. 4(C) and (D) with Fig. 4(E) we see that the peaks in the imaginary part are out of phase, confirming the antiphase behavior as mentioned above.

The number of independent parameters (N_{ind}), which is allowed for the fit procedure [Eq. (4)] of the EXAFS data of the virgin sample is 18 and of the loaded sample is 16. The number of free fit parameters for both fits is 16. This means mathematically that the EXAFS data of the virgin sample are not over fitted. Based upon the results shown in Fig. 4 we feel confident that the analysis of the EXAFS data of the hydrogen loaded sample is reliable. This is further demonstrated in Fig. 5, where the calculated individual EXAFS contributions are shown together with the average experimental noise level. It is clear that the small Gd-Mg contribution loses its significance at $k=5$, while the other elements remain significant up to $k=9$. The gadolinium and hydrogen contributions are most prominent at low-k values. The hydrogen contribution decreases very rapidly in comparison to all the other contributions

In Table III the results of the analysis of the EXAFS data of the hydrogen-exposed GdMg film are given. The Gd-Gd and the Gd-Mg coordination numbers have decreased by 40% and 70%, respectively, compared to those of the as-deposited film. The total coordination around Gd contributing to the metal lattice is 9.5. This number is significantly lower than the total Gd coordination of the unhydrogenated sample. A large increase in the Gd-H coordination number is observed after loading with hydrogen. Also the Gd-O coordination number has increased. Moreover, all interatomic distances have increased under hydrogen loading, except for the Gd-O distance. The degree of disorder, as represented by the Debye-Waller factor, increases for all components except hydrogen. The Debye-Waller factor of hydrogen in the hydrogenated film is much smaller than that of the other constituents, indicating an enhancement of the structural order for the Gd-H coordination.

IV. DISCUSSION

A. Phase separation

From the low Gd-Mg and the high Gd-Gd coordination numbers as shown in Table II, it can be concluded that the GdMg film is already phase separated in the virgin sample. The cubic CsCl structure, expected for the bulk alloy of $Gd_{40}Mg_{60}$, would give a total of eight magnesium nearest neighbors, whereas in the EXAFS analysis a value of 2.7 is found. Since a small amount of hydrogen is also detected in the virgin film we conclude that this phase separation is induced by hydrogen intercalation. From Table III it is clear that phase separation of gadolinium and magnesium is enhanced by exposure to hydrogen. The magnesium concentration in the crystallites is markedly reduced. Clearly the gadolinium forms clusters in which magnesium is present in small amounts. A nanocrystalline composition would explain this result satisfactorily. The fully loaded $Gd_{40}Mg_{60}$ film is amorphous within XRD resolution;[15] hence the nanocrystallites indicated by our experiments must be very small. In electrochemically determined isotherms on GdMg alloy thin films[23] clear plateaus are present, which correspond to single element hydride formation enthalpies. The $Gd_{40}Mg_{60}$ switchable mirror therefore exhibits the same kind of phase sepa-

ration as found for the YMg switchable mirrors in which YH_3 clusters are detected by XRD in the fully loaded state.[4,6] Our EXAFS results directly prove the segregation as proposed in the other studies.

B. Structure

From Table II we see that for the as-deposited film, the total coordination (Gd+Mg) around Gd is almost 12. There are two gadolinium hydride structures that share this coordination number, if one assumes that a fraction of the gadolinium positions is taken by magnesium. The α-Gd hcp geometry would result in 12 nearest neighbors around Gd, at a distance of 3.63 Å.[24] According to the critical temperature of gadolinium,[25] the α state does exist in bulk metal at 77 K. The $\alpha\beta$ phase will also consist mainly of α domains at a very low hydrogen concentration. Therefore the dominant structure detected by EXAFS will be the α-Gd phase. A second possibility would be the β-Gd fcc structure with a nearest-neighbor distance of 3.74 Å.[25] In bulk gadolinium this structure will occur at low hydrogen content. The small nearest-neighbor distances measured for Gd-Gd and Gd-Mg are closer to those of the hcp structure, we therefore conclude that at low hydrogen concentrations the results for the as-deposited film indicate an α-Gd hcp structure.

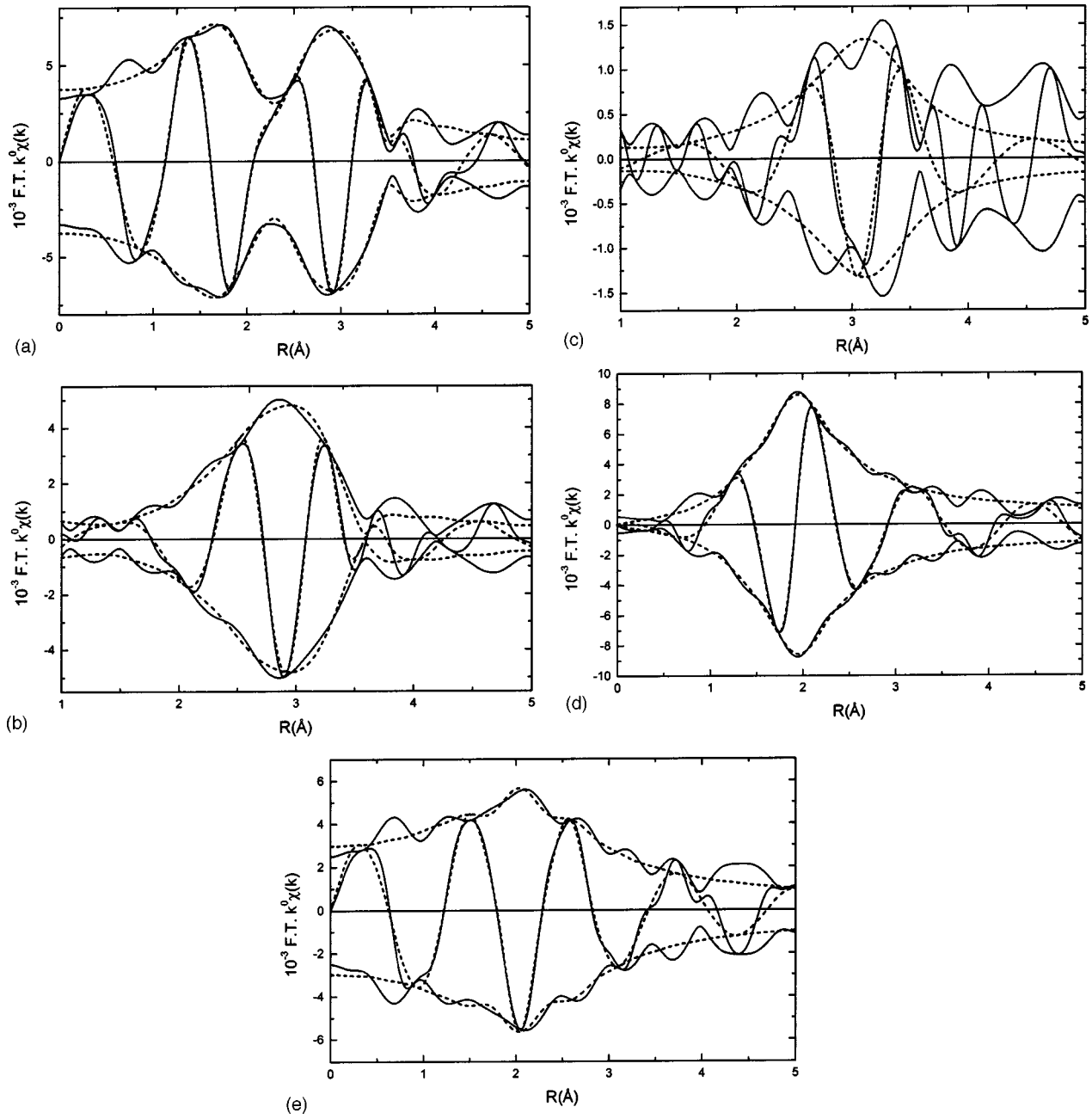

FIG. 4. A Fourier transforms (k^0, $\Delta k = 2.5-10$ Å^{-1}) of raw data (——) and fit (- - -) of the hydrogenated GdMg film. Difference files Fourier transforms in k^0 of raw data (——) and fit (- - -) of (B) Gd-Gd, (C) Gd-Mg, (D) Gd-O, (E) Gd-H.

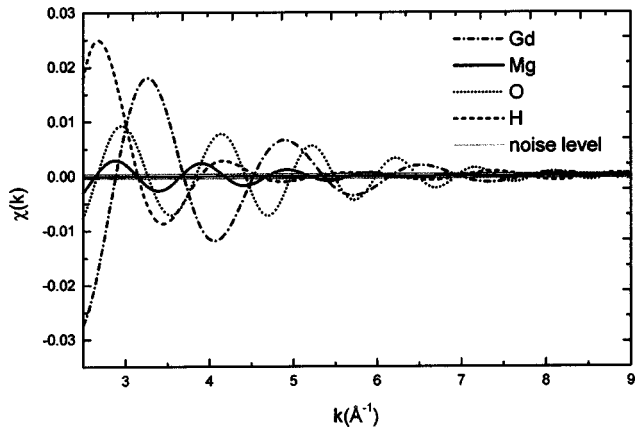

FIG. 5. Calculated $\chi(k)$ of the different atomic contributions to the total fit for the hydrogenated GdMg film. The horizontal line corresponds to the noise level in the raw data.

The small amount of hydrogen, detected in the as-deposited film ($N=1.5$), could be responsible for an expansion of the gadolinium lattice. However, the hydrogen concentration (7%) is very likely too low to induce a hcp to fcc transformation. Therefore the initial hydrogen cannot be responsible for the smaller nearest-neighbor distances than expected. The clamping of the film to the glass substrate very likely induces sufficient strain to reduce the lattice volume slightly.

The reduction of the total coordination (Gd+Mg) around Gd from 12 to 6 after loading with hydrogen is striking. There are again two candidate gadolinium trihydride structures for high hydrogen content: hcp γ-GdH_3 or fcc γ-GdH_3 (in analogy to the YMg results[4]), both of which have 12 nearest neighbors. A face-centered-tetragonal structure for gadolinium would result in four nearest neighbors; this was not found. The hcp gadolinium trihydride structure has a *c*-axis elongation, resulting in a larger distance between the metal planes. Therefore instead of the 12 nearest neighbors in an ideal hcp structure, only the six nearest gadolinium neighbors within the metal plane are expected to be included in the coordination number. Comparing this value with the total coordination (Gd+Mg) of six neighbors present in the hydrogen-loaded sample, we consider it likely that the gadolinium clusters have a hcp structure. However, the Gd-Gd distance of 3.6 Å as observed in the hydrogen-loaded sample, is a little smaller than the distance of 3.73 Å reported for the γ-GdH_3 hcp state.[25]

The total volume expansion of the Gd clusters under hydrogenation cannot be determined since the *c*-axis elongation is not known. The relative expansion of the different elements and their hydrides are provided in Table IV. The lattice parameters from the literature are shown for the metal and fully hydrogenated bulk metal. The relative volume expansion is shown in the last column. The small increase of the nearest-neighbor distance (by only 5%) is in good agreement with the increase of the lattice parameter *a* of 3% for bulk gadolinium. This corresponds to the expansion in the metal plane which again suggests the detection of gadolinium atoms in the metal plane in this EXAFS study. From Table IV it is clear that most of the volume expansion is caused by the *c*-axis elongation upon hydrogenation.

For yttrium clusters in the yttrium magnesium alloy thin films an fcc structure has been reported for magnesium concentrations up to 50%.[6] For the gadolinium alloy with a high magnesium content in the alloy, the total expansion of the film will be larger than that of a pure gadolinium film, since the expansion due to by the formation of magnesium dihydride is much larger than that for gadolinium trihydride (see Table IV). However, with a film composed of separate gadolinium and magnesium clusters, the pressure to which the gadolinium clusters are subjected in the loaded state is related to the amount of surrounding magnesium. In Fig. 6(A) the situation for the low magnesium content is schematically depicted. Since the magnesium clusters are completely surrounded by gadolinium, the pressure will be completely applied to the gadolinium and the magnesium. In Fig. 6(B) it is clear that the magnesium clusters share more surface with each other than with the imbedded gadolinium clusters. The expansion of magnesium will therefore lead mainly to an increase of the pressure on magnesium itself with a resulting increase in the dimensions of the pores. If gadolinium clusters are completely surrounded by magnesium clusters [Fig. 6(B)], the pressure may therefore not increase dramatically. The absence of this additional pressure prohibits the formation of the gadolinium trihydride fcc structure. The pressure dependence of the lattice structure of gadolinium trihydride may be considerably different from that of yttrium trihydride. This could prevent fcc trihydride formation in the case of Gd.

C. Hydrogen

In the Gd trihydride hcp structure each gadolinium atom is surrounded by eight tetrahedral and six octahedral sites.

TABLE III. Gd L_3 edge; fully loaded sample of $Gd_{40}Mg_{60}$/Pd; EXAFS analysis ($2.5<k<10$ Å^{-1}) k^0 weighing.

Absorber-backscatterer	N	R (Å)	$\Delta\sigma^2$ (10^{-3} Å^2)	ΔE_0 (eV)	k variance	
					imaginary	real
Gd-Gd	5.2	3.59	6.0	9.5	0.52	0.25
Gd-Mg	0.6	3.54	18.0	−8.0		
Gd-O	1.0	2.36	8.0	−7.9		
Gd-H	4.1	2.43	2.6	2.4		

TABLE IV. Lattice parameters and volume expansion of bulk Y, Gd, Mg, and hydrides.

	Metal		Fully hydrided		
Element	*a*	*c*	*a*	*c*	Volume expansion
Y (Ref. 25)	3.66	5.77	3.67	6.66 hcp	17%
Gd (Ref. 24)	3.63	5.78	3.73	6.71 hcp	22%
Mg (Ref. 24)	3.21	5.21	8.54	5.71 bcc (Ref. 26)	32%

The tetrahedral sites are located close to the Gd. The hydrogen is considered to be present at the center of each tetrahedron at a distance of 2.3 Å from the Gd.[24] The octahedral interstitial positions are located at a much larger distance and therefore cannot be detected. From the EXAFS analysis the Gd-H coordination is found to be 4. This value is considerably lower than the number of available tetrahedral sites. For yttrium trihydride a HoD_3 structure was initially proposed,[27–29] with a *c*-axis shift of the octahedral hydrogen positions. One-third is located above and one-third below the metal plane. The remaining one-third is positioned within the metal plane. This structure would result in three hydrogen nearest neighbors. However, recent research on the exact location of the hydrogen atoms which are shifted from octahedral positions showed a noncentrosymmetric structure, in which the hydrogen atoms originating from the octahedral positions are differently located on the metal plane ($P6_3cm$ or $P6_3$).[28,30,31] All structures would nevertheless result in three nearest-neighbor hydrogen atoms. On the basis of our experimentally detected Gd-H coordination number of 4, it is highly probable that the nearest-neighbor hydrogen atoms are at the displaced octahedral sites. According to neutron-diffraction experiments on YD_3 the closest tetrahedral deuterium position may be part of the nearest-neighbor hydrogen shell.[27] Hence the remaining detected hydrogen atom can be the closest tetrahedral hydrogen atom. The other tetrahedral hydrogen atoms are likely to be too distant for detection. Since only two structures are plausible, the hydrogen atoms in the octahedral positions or the structure in which the hydrogen atoms are shifted to the metal plane. We conclude that the latter in which the hydrogen atoms are shifted from octahedral positions to the metal plane also holds for GdH_3.

The reduced Debye-Waller factor for the Gd-H coordination in the loaded film is indicative of a high structural order for hydrogen. This is in contrast to the increased structural disorder caused by the lattice expansion of the Gd-Gd and Gd-Mg coordinations constituting the lattice of the GdMg alloy.

With the XAFS techniques, hydrogen has only recently been found[32] as a scattering neighboring atom in the covalent bonding in water. Hydrogen has also been detected indirectly by Pd-Pd lattice expansion using the lens effect in hydrides.[33] Surprisingly, both in the virgin and loaded GdMg films a shell is detected which can only be fitted with hydrogen as a scatterer.

A small amount of oxygen is found in the as-deposited film probably due to oxidation during evaporation. Increased oxidation after loading is clear from Table III. This is unavoidable since lattice transformations induce cracks through which oxygen can diffuse. The recently discovered optical switching properties in NiMg thin films[7] could possibly decrease the oxidation sensitivity of these materials. Based on these experiments we cannot provide information about the nature of the magnesium outside the gadolinium clusters.

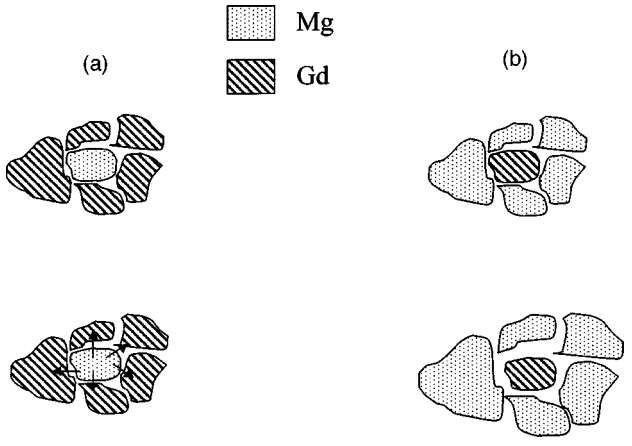

FIG. 6. (A) Magnesium cluster surrounded by gadolinium clusters in a low magnesium content, phase separated film, before and after hydrogenation. The arrows depict the net force by volume expansion. (B) Gadolinium cluster surrounded by magnesium in a high magnesium content, phase-separated film, before and after hydrogenation.

D. Charge transfer

The edge shift of 0.5 eV implies a positively charged gadolinium atom. From the edge shift of 0.9 eV for fully oxidized gadolinium in the gadolinium garnet, we conclude that only a fraction (55%) of the three conduction electrons is transferred to hydrogen atoms. More evidence of partial charge transfer to the hydrogen atoms in yttrium hydrides has been reported. From infrared spectroscopy studies on yttrium thin films[14] an effective charge of $0.5e$ on the hydrogen atoms has been found. An x-ray photoemission spectroscopy study on bulk yttrium hydrides[34] even concludes that no charge is transferred to the hydrogen atoms during the yttrium dihydride to trihydride transition. According to the pressure and transmission-concentration isotherms of a gadolinium thin film,[23] the main optical change occurs when the film is within 10% of the final concentration corresponding to GdH_3, as in the yttrium switchable mirror, while it is known that most of the structural changes occur already on going from the metal to dihydride state. This implies that

charge transfer from the gadolinium atom to the hydrogen atoms may be responsible for optical switching of gadolinium hydrides. The metal-to-insulator transition can therefore be due to a combination of two effects: (i) structural change (i.e., lattice expansion) and (ii) charge transfer to the hydrogen atoms. This would be consistent with evidence for a charged hydrogen atom, found in lateral electromigration experiments by van der Molen *et al.*[35] Since the optical changes during the electromigration experiments are only induced by the reversibly loaded hydrogen, i.e., one-third of the hydrogen content, it is not necessary that all charge is transferred to the other hydrogen positions.

V. CONCLUSIONS

The $Gd_{40}Mg_{60}$ hydride switchable mirrors are phase segregated in the as-deposited film and segregation is enhanced by hydrogen loading. A hcp lattice structure for the small gadolinium clusters could be established both for the as-deposited and the hydrogenated film, suggesting nanocrystallinity. Hydrogen could be detected by EXAFS as a scatterer in a solid-state material. The Gd-H coordination number found in the hydrogenated film suggests a structure in which the octahedral hydrogen atoms are shifted to the metal plane in gadolinium trihydride, also previously reported for yttrium trihydride. Only 55% of the available charge is transferred to the hydrogen atoms. This may be of crucial importance for the main optical transition.

ACKNOWLEDGMENTS

The authors would like to thank Philips Research, P. van der Sluis, and A.-M. Janner for stimulating discussions, and E. M. H. Evens and J. M. Kerkhof for preparation of the samples. Discussions with R. Griessen and A. Remhof from the Vrije Universiteit Amsterdam are greatly appreciated. The work described here was supported by the Council for Chemical Sciences (CW), with financial aid from the Netherlands Organization for Scientific Research (NWO) and the Netherlands Foundation for Technical Research (STW).

*Present address: Laboratory for Technical Chemistry, ETH Hönggerberg, Zurich, Switzerland.

†Present address: Laboratoire de Science des Matériaux, Université Paris-Sud XI, Paris, France.

[1] J. N. Huiberts, R. Griessen, J. H. Rector, R. J. Wijngaarden, J. P. Dekker, D. G. de Groot, and N. J. Koeman, Nature (London) **380**, 231 (1996).

[2] P. van der Sluis and V. M. M. Mercier, Electrochim. Acta **46**, 2167 (2001).

[3] P. van der Sluis, M. Ouwerkerk, and P. A. Duine, Appl. Phys. Lett. **70**, 3356 (1997).

[4] D. G. Nagengast, A. T. M. van Gogh, E. S. Kooij, B. Dam, and R. Griessen, Appl. Phys. Lett. **75**, 2050 (1999).

[5] J. Isidorsson, I. A. M. E. Giebels, E. S. Kooij, N. J. Koeman, J. H. Rector, A. T. van Gogh, and R. Griessen, Electrochim. Acta **46**, 2179 (2001).

[6] S. J. van der Molen, D. G. Nagengast, A. T. M. van Gogh, J. Kalkman, E. S. Kooij, J. H. Rector, and R. Griessen, Phys. Rev. B **63**, 235116 (2001).

[7] T. J. Richardson, J. L. Slack, R. D. Armitage, R. Kostecki, B. Farangis, and M. D. Rubin, Appl. Phys. Lett. **78**, 3047 (2001).

[8] R. Griessen, Europhys. News **32** (2), 42 (2001).

[9] M. Mannsmann and W. E. Wallace, J. Phys. (Paris) **25**, 454 (1964).

[10] K. K. Ng, F. C. Zhang, V. I. Anisimov, and T. M. Rice, Phys. Rev. B **59**, 5398 (1999).

[11] P. J. Kelly, J. P. Dekker, and R. Stumpf, Phys. Rev. Lett. **78**, 1315 (1997).

[12] P. van Gelderen, P. A. Bobbert, P. J. Kelly, and G. Brocks, Phys. Rev. Lett. **85**, 2989 (2000).

[13] P. van Gelderen, P. J. Kelly, and G. Brocks, Phys. Rev. B **63**, 100301 (2001).

[14] M. Rode, A. Borgschulte, A. Jacob, C. Stellmach, U. Barkow, and J. Schoenes, Phys. Rev. Lett. **87**, 235502 (2001).

[15] P. van der Sluis, Appl. Phys. Lett. **73**, 1826 (1998).

[16] F. W. Kampers, T. m. J. Maas, J. van Grondelle, P. Brinkgreve, and D. C. Koningsberger, Rev. Sci. Instrum. **60**, 2635 (1989).

[17] M. Vaarkamp, J. C. Linders, and D. C. Koningsberger, Physica B **208**, 159 (1995).

[18] B. K. Teo, *EXAFS: Basic Principles and Data-analysis* (Springer, New York, 1986).

[19] J. W. Cook, Jr. and D. E. Sayers, J. Appl. Phys. **52**, 5024 (1981).

[20] A. L. Ankudinov, B. Ravel, J. J. Rehr, and S. D. Conradson, Phys. Rev. B **58**, 7565 (1998).

[21] D. C. Koningsberger, B. L. Mojet, G. E. van Dorssen, and D. E. Ramaker, Top. Catal. **10**, 143 (2000).

[22] D. C. Koningsberger, Jpn. J. Appl. Phys., Part 1 **32**, 877 (1993).

[23] M. Di Vece, S. J. M. Zevenhuizen, and J. J. Kelly, Appl. Phys. Lett. **81**, 1213 (2002).

[24] D. R. Lide and H. P. R. Frederikse, *Handbook of Chemistry and Physics* (CRC, Boca Raton, 1993–1994).

[25] P. Vajda, in *Handbook on the Physics and Chemistry of Rare Earth*, edited by K. A. Gscheidner and L. Eyring (Elsevier, Amsterdam, 1995), Vol. 20.

[26] F. H. Ellinger, C. R. Holley, Jr., B. B. Mcinteer, D. Pavone, R. M. Potter, E. Staritzsky, and W. H. Zachariasen, J. Am. Chem. Soc. **77**, 2647 (1955).

[27] T. J. Udovic, Q. Huang, and J. J. Rush, J. Phys. Chem. Solids **57**, 423 (1996).

[28] O. J. Zogal, W. W. Wolf, P. Herzig, A. H. Vuorimäki, and E. E. Ylinen, Phys. Rev. B **64**, 214110 (2001).

[29] A. Remhof, G. Song, Ch. Sutter, A. Shreyer, R. Siebrecht, and H. Zabel, Phys. Rev. B **59**, 6689 (1999).

[30] T. J. Udovic, Q. Huang, R. W. Erwin, B. Hjörvasson, and R. C. C. Ward, Phys. Rev. B **61**, 12 701 (2000).

[31] H. Kierey, M. Rode, A. Jacob, A. Borgschulte, and J. Schoenes, Phys. Rev. B **63**, 134109 (2001).

[32] K. R. Wilson, J. G. Tobin, A. L. Ankudinov, J. J. Rehr, and R. J. Saykally, Phys. Rev. Lett. **85**, 4289 (2000).

[33] B. Lengeler, Phys. Rev. Lett. **53**, 74 (1984).

[34] A. Fujimori and L. Schlapbach, J. Phys. C **17**, 341 (1984).

[35] S. J. van der Molen, M. S. Welling, and R. Griessen, Phys. Rev. Lett. **85**, 3882 (2000).